BioNanoScience (2025) 15:250
https://doi.org/10.1007/s12668-025-01857-y

RESEARCH

Preparation of Silk Fibroin Nanofibers Containing 5-Fluorouracil for pH-Sensitive Drug Delivery and Synergistic Cancer Therapy

Mehdi Fathi[1,2] · Faride Ranjbari[3] · Majid Joudi[4] · Payam Farazmand[4] · Effat Iranijam[4] · Hamed Haghi-Aminjan[5] · Farzneh Fathi[5]

Accepted: 6 February 2025

Abstract

Every year, over one million instances of gastric carcinoma receive diagnoses on a global scale. The objective of the present study was to explore the synergistic impact of silk fibroin nanofibers (SFNFs) containing the pharmaceutical agent 5-fluorouracil (5-FU) in managing gastric cancer, centering on the MKN-45 cell line. For this study, we produced a nanofiber structure using a ratio of 1:5 of 5-FU to SFNFs. We analyzed the SFNFs using Fourier-transform infrared spectroscopy (FT-IR), UV spectroscopy, and scanning electron microscopy (SEM). The effect of pH on drug release was measured using the dialysis method. After this, assessments of cellular toxicity and the transcription of apoptotic (Bax, Bcl-2, and p53) and autophagic (Beclin-1 and LC3-II) genes were conducted utilizing MTT and PCR methodologies. In summary, SFNFs showed excellent controlled 5-FU delivery at different pHs and the amount of 5-FU release has increased as the pH decreases. Moreover, the merging of nanofibers with 5-FU substantially augmented the transcription of apoptosis and autophagy-associated genes, after 3 and 5 days (P-value < 0.05). It seems that the anticancer mechanism of 5-FU entails stimulating the expression of the mentioned genes, a process that can be facilitated by the presence of SFNFs.

Keywords Silk fibroin nanofiber · 5-Fluorouracil · PH-sensitive · Drug delivery

✉ Farzneh Fathi
farzan_fathi2000@yahoo.com; f.fathi@arums.ac.ir

[1] Department of Esthetic and Restorative Dentistry, School of Dentistry, Ardabil University of Medical Sciences, Ardabil, Iran

[2] Department of Dental Biomaterials, School of Dentistry, Ardabil University of Medical Sciences, Ardabil, Iran

[3] Women's Reproductive Health Research Center, Tabriz University of Medical Sciences, Tabriz, Iran

[4] Department of Internal Medicine (Hematology Division), School of Medicine, Ardabil University of Medical Sciences, Ardabil, Iran

[5] Pharmaceutical Sciences Research Center, Ardabil University of Medical Sciences, Ardabil, Iran

Published online: 26 February 2025

1 Introduction

Several drug delivery systems have been developed in recent years to administer multiple medications and to release them in a regulated manner to improve their effectiveness. Considering that most anti-cancer drugs spread non-specifically throughout the body and are consumed by all cells, the use of an efficient and stable drug can be very effective in reducing the side effects of drugs and their accumulation in the treated area. Therefore, the best-promising strategy could be controlled drug release at the tumor site at a specific time by carriers [1]. These systems provide many benefits, namely increasing the bioavailability of medicinal products by reducing degradation rates, improving cellular uptake, enabling targeting and control of drug release as well as minimizing side effects [2, 3]. The use of degradable nanostructures as an appropriate material due to their limitations in low drug loading and rapid drug release caused by their large pores and high water content makes them unsuitable [4, 5].

Electrospinning is a versatile technique for fabricating continuous, nanofibers from a wide range of polymeric materials like Poly(lactic-co-glycolic acid) (PLGA), polyvinyl alcohol (PVA), polycaprolactone (PCL), chitosan, etc. [6–8]. These nanofibers exhibit unique properties such as high surface area-to-volume ratio, 3D topography, tunable porosity, and flexible surface functions were introduced as a good alternative for targeted drug delivery [9, 10]. Usual drug types, like tablets, capsules, and injections, are incomplete when used for targeted and smart drug delivery. To overcome these limitations, nanofibers have been disclosed as novel nanomaterials to offer improved targeted drug delivery, low toxicity and prolonged drug release manner [11, 12]. The use of natural biopolymers for drug delivery systems has garnered significant attention due to their inherent biological and physicochemical properties. Silk fibroin (SF) is an FDA-approved, biocompatible, and biodegradable natural polymer that possesses exceptional mechanical qualities. It is a compelling choice for drug delivery applications [13, 14]. The β-sheet structure of this polymer determines its mechanical properties and increases its hydrophobicity. This polymer is made up of six repeating sequences of hydrophobic residues: Gly-Ala-Gly-Ala-Gly-Ser [4, 15]. Due to having thixotropic properties by SF, they become shear-thin and flow during injection, and immediately after injection, they return to solid form. As a result, these structures can be used in most chemotherapy due to their injectability [16, 17]. The loading efficiency of 5-fluorouracil (5-FU), as an anti cancer drug, in nanostructures, specifically chitosan and alginate nanoparticles, is below 30%. Furthermore, increasing the drug/polymer ratio leads to a decrease in loading efficiency, even if it was initially higher. This means that we need to make a novel matrix that can hold a lot of drugs consistently and in large amounts to load small molecules that dissolve in water [18, 19]. Given that the pH in normal cells is higher than that of inflammatory and cancerous cells, it is 7.4 in normal cells and 6.4 in inflammatory cells, so the anticancer drug delivery system of pH-triggered nanoparticles have received a lot of attention for achieving the better effectiveness [20, 21]. In 2018, Ning Sun et al. fabricated a porous silk fibroin to study the release of doxorubicin, then to research the drug release behavior of silk nanoparticles at different pHs, the concentration of the released drug was investigated [22]. They showed that the release of the drug by the porous silk fibroin in the acidic environment and subsequently in cancer cells will be enhanced.

In this study, we prepared nanofibers of silk fibroin by the electrospinning method for loading 5-FU in this structure. SFNFs in vitro cumulative 5-FU release profiles at different pHs were studied. We analyzed the SFNFs using FT-IR, UV spectroscopy, and SEM. The effect of pH on drug release was measured using the dialysis method. The cytotoxicity study was conducted for all the SFNFs with/without 5-FU on the MKN-45 cell line to determine their toxicity on the gastric cancer cells and develop a suitable carrier of 5-FU. After this, assessments of the transcription of apoptotic (Bax, Bcl-2, and p53) and autophagic (Beclin-1 and LC3-II) genes were conducted by PCR method. The objective of the present study is to develop a suitable pH-responsive carrier of 5-FU which can effectively work in a cancerous environment to fight against gastric-related cancer.

2 Materials and Methods

2.1 Materials and Methods

Silk cocoons were purchased from the local market of Tabriz (Tabriz, Iran). Sigma-Aldrich provided 5-FU, dialysis bag with cut-off 8000 kDa, lithium bromide (LiBr), sodium carbonate, ethanol, sodium hydroxide, 3-(4,5-dimethylthiazol-2-yl)−2,5- diphenyl-tetrazolium bromide (MTT), dimethyl sulfoxide (DMSO), sodium chloride, potassium chloride, di-sodium hydrogen phosphate, di-sodium hydrogen phosphate di-hydrate, hydrochloric acid (37%) and all other reagents which were of analytical-reagent grade without any additional purification. The Pastor Institute in Iran prepared the MKN-45 cell line.

2.2 Preparation of Silk Fibroin (SF)

We fragmented the dried silk cocoons into small pieces and immersed them in a sodium carbonate solution

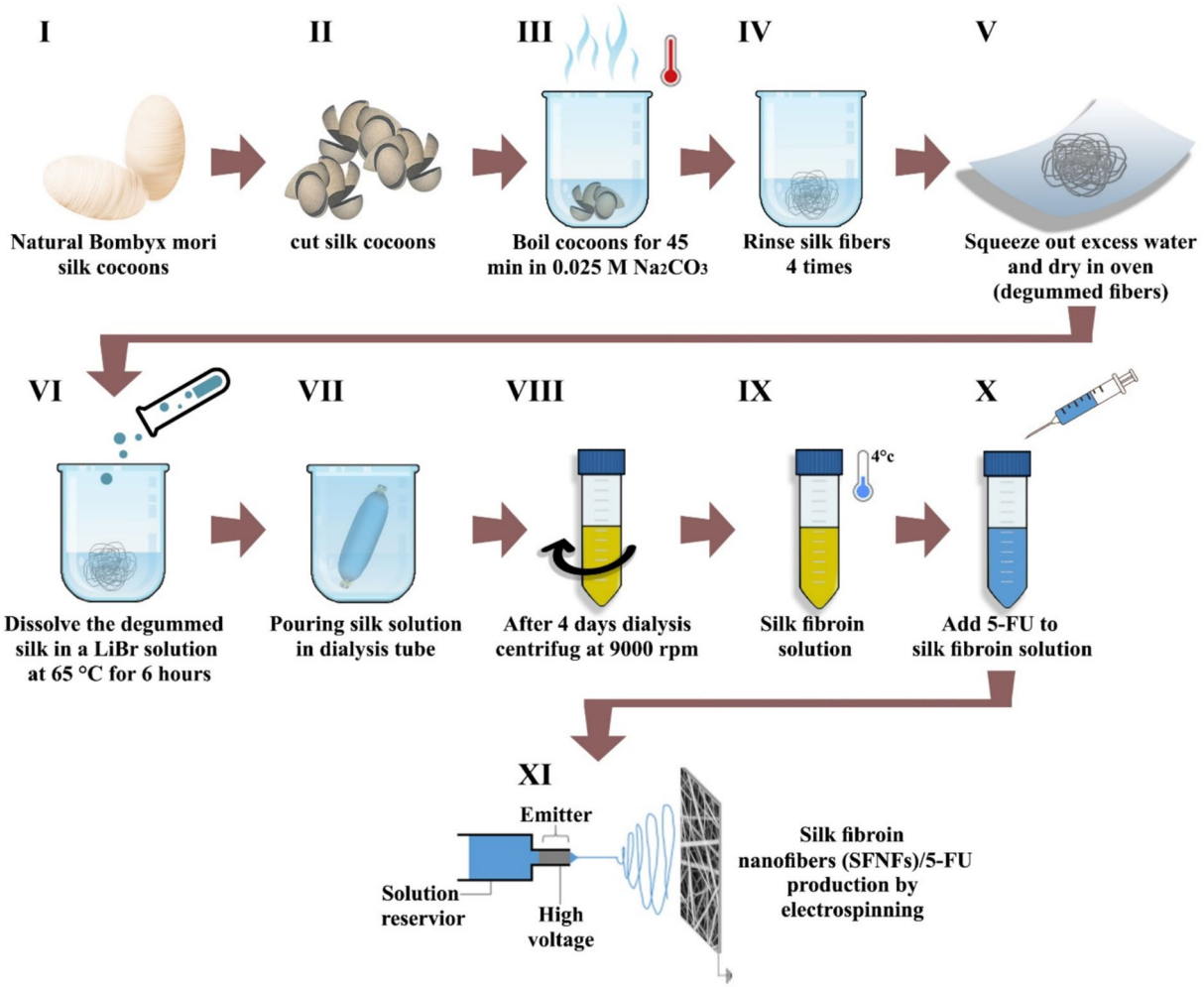

Scheme 1 Schematic illustration of steps of SFNFs preparation **I** to **IX**, and SFNFs/ 5-FU solution along with electrospinning **IX** to **XI**

(0.025 M), boiling and stirring vigorously for 45 min. The entire volume was regularly rinsed with distilled water (DW) to remove the sericin molecules and then dried for 24 h in an oven at 50 °C. Next, we dissolved the degummed silk in a LiBr solution at 65 °C for 6 h. The SF solution was dialyzed in a cellulose bag-based dialysis tube with a molecular cutoff of 8000 KDa to remove LiBr salts in a cellulose bag against distilled water. We carried out the dialysis against distilled water for 4 days, refreshing the water every 5 h. We carried out this process to extract salt molecules from the solution. Finally, we centrifuged the prepped SF solution for 25 min at a temperature of 4 °C and a speed of 9000 revolutions per minute [23, 24]. We store the resulting SF solution at 4 °C for further analysis. In Scheme 1, the schematic illustration of the preparation of the SF solution from I to IX is shown.

2.3 Preparation of the Spinning Solution and Electrospinning

The obtained solution of SF was directly concentrated to generate about 30% of the fibroin solution by weight with slow stirring at 55°C. Then, at a 20% (W/W) of 5-FU weight to SF weight, we added the drug to the solution, approximately equivalent to 100 mg of 5-FU and the control group, which did not have 5-FU. With constant stirring, the SF solution was prevented from whirling into a gel form during the concentrating procedure. Then, the prepared solution was placed in the electrospinning machine for 6 h and electrospun structures were obtained. We used an electrospinning apparatus from Fanavaran Nano-Meghyas (FNM Co. Ltd. Iran). We conducted the electrospinning process under identical conditions, ensuring a temperature below 20 °C and a

relative humidity of 12%. We loaded 1000 l of SF solutions into a 1-mL syringe, fitted with a specific-sized stainless-steel needle, and connected it to a voltage power source. We applied a voltage ranging from 12 to 20 kV at the tip to generate spinning solutions. We deposited the electrospun SFNFs onto aluminum foil at a distance of 15 cm from the capillary tip (Scheme 1, IX—XI).

2.4 SEM Images

The size and uniformity of both pure and electrospun SFNFs were analyzed by comparing the scanning electron microscope (SEM) images of each fibroin sample obtained using the Tescan MIRA3 FEG-SEM.

2.5 Fourier-Transform Infrared Spectroscopy (FTIR)

The FTIR spectra were utilized to determine the molecular structure of 5-FU, SFNFs, and nanofibers loaded with 5-FU. The FTIR spectra were obtained using a Nicolet FT-IR instrument from Thermo Scientific, located in Madison, USA. The scans were recorded in the range of 4000–500 cm^1, and potassium bromide (KBr) pellets were used. The tabs were organized using a powder ratio of 10% (w/w) SFNFs/KBr.

2.6 *In Vitro* Drug Release pH-Dependent 5-FU from the Electrospinning Silk Fibroin (SF-Loaded 5-FU)

To examine the release of 5-FU in a laboratory setting, SFNF loaded with 5-FU was placed in a suspension of 5 mL of PBS solution at room temperature. The suspension was stirred slowly and consistently. Three PBS solutions with varying pH values (7.5, 6.5, and 5.5) were prepared using HCl or NH_3 and studied for 24 h to observe their effects on diverse biological scenarios. Briefly, the 100-mg SFNFs were sealed in a dialysis tube (12000 kDa), which was further spread in a 10 mL PBS solution. At suitable breaks, 100 µL release medium was removed for the spectral test, and the same volume of fresh PBS solution was replaced. The released 5-FU molecules in the buffer were measured by an ultraviolet (UV) spectrophotometric device (bioteck) at 230–400 nm. The cumulative release percentage of the 5-FU was calculated according to the reference [25].

2.7 Cell Viability Assay

By measuring the cell viability using the MTT test, the cytotoxic effects of 5-FU-loaded SFNFs and SF on MKN cells were evaluated. The Iranian Pasteur Institute produced these cell lines. After 96-well cell culture microplates were filled with cells at a density of 4×10^4 cells/mL, the plates were incubated at 37 °C in a humidified atmosphere with 5% CO_2. The cells were separated using a 0.25% Trypsin–EDTA (Gibco) solution when they reached 75–80% confluence. We used pure SFNPs at a concentration of 20 µg/µL as a reference point and 5-FU-loaded SFNPs to measure the reactivity of cells to dangerous chemicals. Following a 5-day incubation period, the culture medium was removed from every well and replaced with 180 µL of fresh medium. The wells were filled with 20 µl of MTT solution, and the plate was incubated at 37 °C. For 3 and 5 days, the cells were cultivated in a CO_2 incubator with SFNPs loaded with 5-FU and pure SFNPs. After incubation, a serum-free medium containing 1 mg/mL MTT was added to the culture media containing medications, and the mixture was cultured for an additional four hours. After adding DMSO, the absorbance of the cell surface on a well plate was measured at 630 nm using an ELISA microplate reader. As a positive control, the MKN-45 cells that were not given any treatment were shown to be 100% viable.

2.8 Real-Time PCR for Measuring the Expression of Apoptosis and Autophagic Genes

Real-time PCR and specific primers were used to evaluate gene expression of p53, p38, p16, p21, TNF-α, IL-1, IL-6, and MMP-2. Initially, mRNA was extracted from the cells using an appropriate kit method. We employed a Nano-Drop UV–vis spectrophotometer (Thermo Fisher Scientific, CA) to determine the concentration of RNA. Afterward, complementary DNA (cDNA) was generated using an iScript cDNA synthesis kit. The aforementioned genes were amplified with specific primers that were designed using the NCBI Primer design tool and purchased from Eurogenes Genomics (Eurogenes Genomics, Germany). In the end, a real-time polymerase chain reaction (PCR) was performed using a SYBR green master mix on a Light Cycler 96 device (Roche Applied Sciences, USA). To do the analysis, the cycle number (Ct) of each reaction was acquired and subsequently standardized using ACTB mRNA. The gene expression level was quantified as $2^{-\Delta\Delta Ct}$. In this study, the following specific primers were used:

ACTB F : AAAACTGGAACGGTGAAGGT
ACTB R : AACAACGCATCTCATATTTGGAA
p53 F : CGTGTGGAGTATTTGGATGAC
p53 R : TTGTAGTGGATGGTGGTACAGTC
Bax F : CCCGAGAGGTCTTTTTCCGAG
Bax R : TGGTTCTGATCAGTTCCGGC
Bcl – 2 R : CCCGGTTATCGTACCCT
Bcl – 2 F : GTTCCGCGTGATTGAAGA
Beclin 1 F : TCTGGCACAGTGGACAGTTT
Beclin 1 R : ATGGAGCAGCAACACAGTCT
LC – 3 R : GCTCATGTTGACATGGTCCG

The differences between groups were assessed using GraphPad Prism 8 software (GraphPad Company, San Diego, CA, USA) by employing analysis of variance (Tukey test) and/or a non-parametric test (Bonferroni test). Statistically significant values were defined as $P < 0.05$.

3 Results and Discussion

3.1 Fourier-Transform Infrared Spectroscopy (FTIR)

Figure 1 exhibits the FT-IR spectra of 5-FU, pure SFNFs, and SFNFs loaded with 5-FU. The 5-FU spectra (black curve in Fig. 1) exhibited characteristic vibration bands at 870, 1247, 1347, and 3071 cm^{-1}. The vibration bands mentioned correspond to the functional groups of C-H (bend), C-F (stretch), C-N (stretch), and N–H (stretch), respectively. The FTIR spectroscopy reveals the carbon–fluorine bond stretching in the range of 1000 to 1360 cm^{-1}. The sensitivity of the stretching frequency to other groups within the structure of the molecule is directly connected with its extensive value. The wavenumber position of the absorption bands of the amide groups can be utilized to ascertain the conformational arrangement of SFNFs. The β-sheet arrangements in silk fibroin structures are characterized by absorption bands falling within the range of 1643 cm^{-1}. The existence of an amide group (indicated by the C = O stretching band) was verified by the vibration band observed at 1652 cm^{-1} in the SF spectrum (red curve in Fig. 1). The structure of amide I is observed as a random coil at the vibration band position (1652 cm^{-1}) in the SF spectrum. The identification of 5-FU in the structure of SFNFs was confirmed by the appearance of three distinct peaks in the spectrum of the 5-FU-loaded SF nanofiber (red curve) at 813 cm^{-1} (corresponding to the C-H functional group) and 1243 cm^{-1} (corresponding to the C-F functional group). The spectra within the 3100–3600 cm^{-1} region can exhibit the hydrogen bonds formed between 5-FU and SFNFs.

3.2 SEM Analyses

Figure 2 shows the SEM images of the SF before and after electrospinning and their diameter distribution. The nanofibers all have very similar surface morphologies. These morphologies consist of random alignments of fibers that are uniform and without beads, which indicates the fibers formed very unbroken and even [27]. The size and shape of the SF before electrospinning were with diameters of near 2 µm (Fig. 2a). In contrast, after electrospinning, the regenerated SF has changed to a smaller size with diameters of nearly 100–150 nm on average. The size of the freshly manufactured SFNFs was determined to be optimal, with an average diameter of 125 nm.

Polymer concentration and electric current during electrospinning is a key factor that affects the final fiber morphology [26–28]. Generally, extremely high polymer concentration may lead to the electrospinning process being impossible due to high viscosity, whereas low concentration or high voltage results in fibers with beads. The observed beads in SFNFs without 5-FU, also can as a result of these issues (Fig. 2b). But in the SEM image of SFNFs with 5-FU the number of beads decreased, which indicated the proper situation of the electrospun solution (Fig. 2c).

3.3 Loading Result and *In Vitro* pH-Dependent Release Study of 5-FU from SFNFs

The quantity of 5-FU enclosed within the SFNFs was measured in triplicate by UV–Vis spectroscopy and drawing the standard curve (concentration of 5-FU as the abscissa and the absorbance as the ordinate). To determine the encapsulation efficiency (EE) the amount of 5-FU loading into the SFNFs was calculated by subtracting the amount of free drug present in the supernatant from the total amount of drug used to prepare the structure. The quantity of free drug was measured spectrophotometrically at a wavelength of 265 nm.

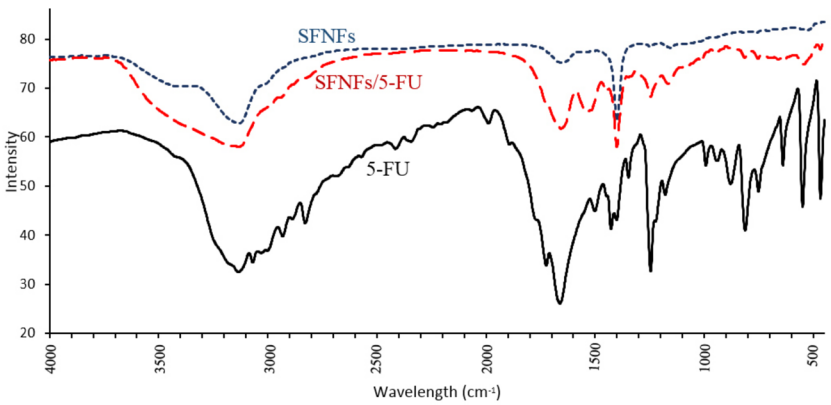

Fig. 1 The FTIR spectra of pure silk fibroin (blue curve), 5-FU loaded SFNFs (red curve) and 5-Fluoracil (black curve)

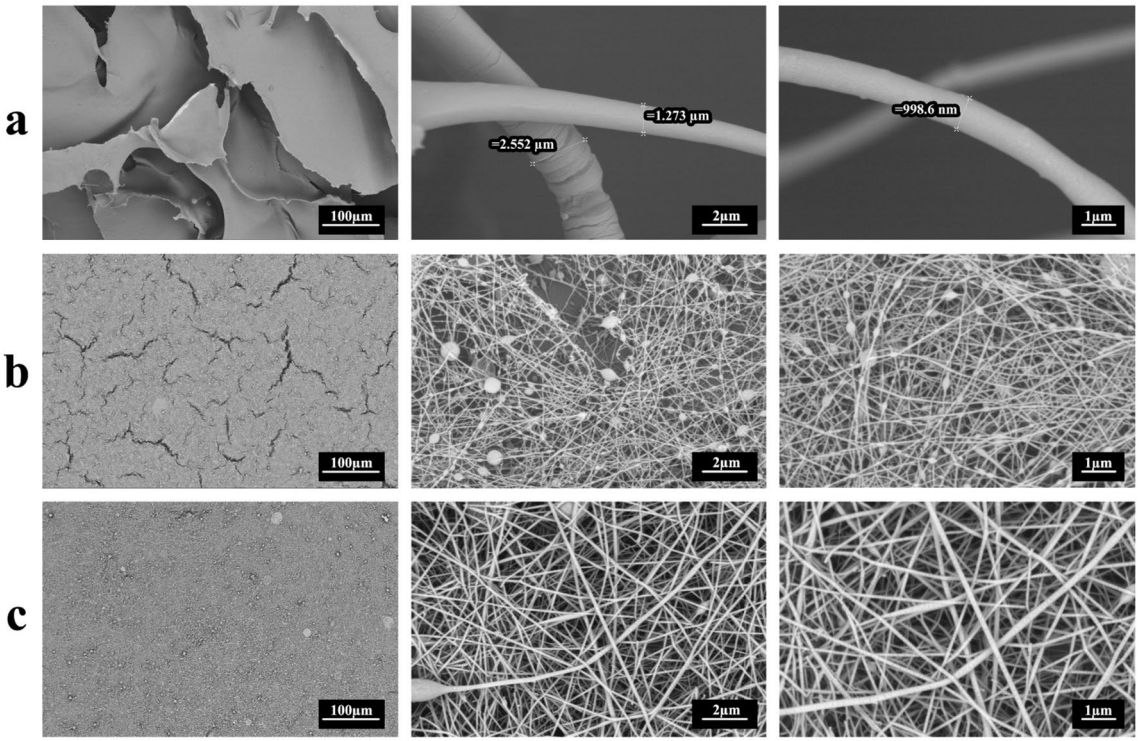

Fig. 2 SEM images Silk fibroin: **a**) before electrospinning, **b**) after electrospinning without 5-FU, **c**) after electrospinning with loaded 20% 5-FU

The LV and EE of the 5-FU in SFNFs structures were considered using the following formula:

$$Loading\ value\ (LV) = \frac{The\ mass\ of\ entrapped\ 5-FU\ (mg)}{The\ mass\ of\ 5-FU\ loaded\ nanofibers\ (mg)} \times 100$$

$$Encapsulation\ efficiency\ (EE) = \frac{Total\ amount\ of\ 5-FU\ drug - Amount\ of\ free\ 5-FU\ drug\ (mg)}{Total\ amount\ of\ 5-FU\ drug\ (mg)} \times 100$$

Also, using a UV-spectrophotometer measured the released 5-FU drug at 265nm using the following equation:

$$Release\ (\%) = \frac{Released\ amount\ of\ 5FU}{Total\ amount\ of\ encapsulated\ 5FU} \times 100$$

The maximum absorption length of the 5-FU medicine was determined by analyzing the absorption spectra in the 200–400 nm range (Fig. 3). The analysis revealed that the drug's greatest absorption occurs at 265 nm. The polymer and pharmaceutical quantities were kept constant, with a drug-to-polymer ratio of 1:5 and the LV and EE for this ratio was 42.2 ± 0.24 and 71 ± 0.45 respectively. The intended pharmaceutical compound was likewise discharged from the nanofiber framework within this specific range of wavelengths. The release of 5-FU was investigated at different pH

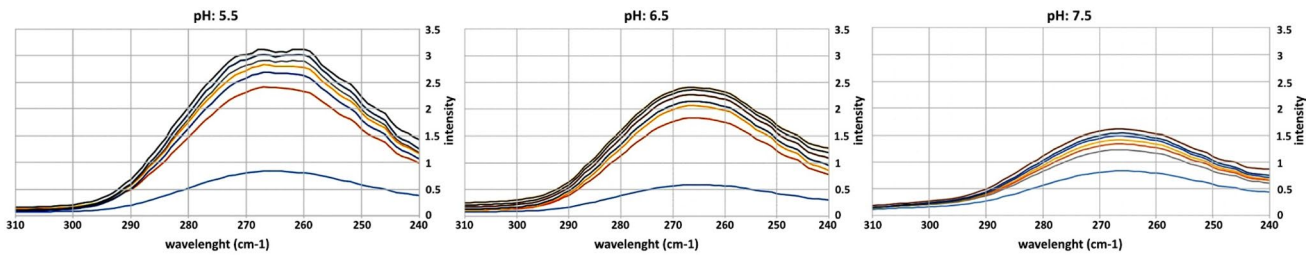

Fig. 3 The relevant absorption spectrum of delivery of 5-FU loaded in SFNFs at different pH situations

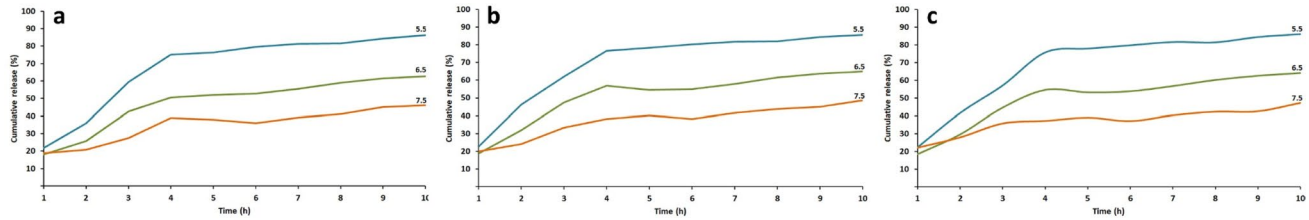

Fig. 4 The release profile of 5-FU from 5-FU loaded SFNFs (at ratios 1:5) at three pH (5.5,6.5 and 7.5) in different wavelengths, **a**) 260 nm, **b**) 265 nm and **c**) 270 nm

levels using three wavelengths close to the maximal values: 260, 265, and 270 nm. At a pH of 5.5, the highest loading content was achieved. When a β-sheet structure is present in the SFNFs, 5-FU does not stick together or move around as much. When the silk fibroin's β-sheet content increases, drug encapsulation within the nanoparticles is enhanced when the β-sheet content in the SF increases. The investigation of in vitro drug release involved measuring the amount of 5-FU released and evaluating its absorption. As the pH has risen, there has been an increase in drug release. Research has shown that over time, the release of a substance increases gradually, continuing to climb throughout the initial hours until reaching a plateau.

As shown in Fig. 4, with the decrease in pH, the drug release from SFNFs has also increased. Hydrogels are three-dimensional, cross-linked polymer networks that can absorb and retain significant amounts of water or other solvents [29–31]. When the pH of the environment changes, it can affect the ionization of the functional groups in this structure. As a result, the hydrogel may swell or contract in response to these pH changes and be effective in releasing various drugs [32]. Also, many nanofibers contain acidic or basic functional groups (such as carboxyl groups or amino groups) that can undergo ionization in response to pH changes [33–35]. When the pH decreases (becomes more acidic), acidic groups may be protonated, leading to increased positive charges in the hydrogel-based nanofibers. Conversely, when the pH increases (becomes more basic), the basic groups may become more deprotonated, leading to an increase in negative charges in the nanofibers. This issue may play a role in their release due to the load of the effective substance [36]. On the other hand, changes in charge density due to pH changes can lead to electrostatic repulsion between polymer chains. This expulsion can cause swelling of the nanostructure and create pores or cracks in its arrays. These pores allow the diffusion and release of drug molecules that are enclosed inside the SFNFs. On the other hand, increasing the porosity and swelling of the nanofibers at lower pH levels facilitates the diffusion of drug molecules out of the SFNFs matrix. This effect leads to a higher rate of release of the drug into the surrounding environment [37]. However, it is equally remarkable to observe that the increase in drug release reaches a constant value over time. The enhancement of drug release with decreasing pH is a well-documented phenomenon in many drug delivery systems, especially those using nanostructure matrices [38–40]. For example, recently D Dhar et al. reported chitosan-coated nanoparticles for the pH-sensitive and sustained delivery of 5-FU in vitro [41]. The result of this study showed that the maximum 5FU release was near 40% within the acidic media. But our study exhibited that more release in the same situation (80%). The primary innovation of developed SFNFs/5-FU lies in the pH-sensitive nature of the system. This targeted release enhances drug efficacy. Also, by limiting drug release to the tumor site, the risk of systemic toxicity associated with conventional chemotherapy can be significantly reduced.

3.4 In Vitro Cytotoxicity

The viability of MKN cells in the presence of 5-FU loaded SFNFs and SF was investigated to evaluate the cytotoxic. Figure 5 shows the substances' cytotoxicity in the MKN-45 cell line. The pure self-assembled nanofibrous structures did not exhibit any cytotoxic effects on the cell line, while the SFNFs loaded with drugs showed significant cytotoxicity. The study looked at whether the MKN-45 cell line could grow on this substrate. There were two groups: one that was treated with 5-FU and the other that was not. Also,

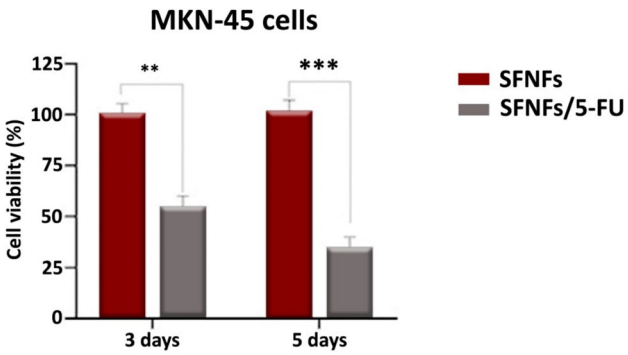

Fig. 5 Cytotoxic activity of 5-FU loaded SFNFs and free SFNFs on MKN-45 calculated by ANOVA (*$P \leq 0.001$)

the effect of SFNFs on cell viability was investigated in two periods of 3 days and 5 days after treatment. The results obtained are as follows: On the third day, the life of cells treated with 5-FU along with nanofibers carriers was significantly reduced compared to the group treated only with nanofibers (P-value < 0.001). On the fifth day, the life of cells treated with 5-FU along with SFNFs carriers was significantly reduced compared to the group treated with just SFNFs (P-value < 0.001).

3.5 Investigation of the Expression of Apoptosis Bax, Bcl-2, and p53 Genes

The number of genes related to apoptosis of the MKN-45 cell line on the SFNFs substrate was investigated in two groups treated with 5-FU and without treatment. Also, the effect of SFNFs on the expression of the genes of the apoptotic pathway in two periods of 3 days and 5 days after the treatment was investigated. The results are presented in Fig. 6. On the third day, Bax and p53 gene expression increased in cells treated with a 5-FU/SFNFs carrier compared to the group treated with just SFNFs, which indicates an increase in apoptosis (P-value < 0.05). When compared to the group that only got the SFNFs, the group that got 5-FU along with the carrier showed a small drop in Bcl-2 gene expression after three days. Nevertheless, this discrepancy did not reach statistical significance (P-value > 0.05). On the fifth day, there was a substantial drop in Bcl-2 expression in the group treated with SFNFs/ 5-FU carriers compared to the group treated with nanofibers alone. This decrease was statistically significant, with a P-value of less than 0.05. When cells were treated with 5-FU/SFNFs carriers, Bax and p53 gene expression increased. Moreover, initial investigations indicate that 5-FU induces deadly consequences in colon cancer cells by modifying Bcl-2 family proteins [42]. Susan et al. also showed that 5-FU can increase the expression of p53 and thereby lead to an increase in apoptosis [43]. Additionally, it appears that 5-FU stimulates the pro-apoptotic Bcl-2 family members (Bax and Bak), causing the release of cytochrome c. This release facilitates caspase-9 activation by attaching to Apaf-1. Upon activation, caspase 9 undergoes cleavage and subsequently activates caspase 3. Caspase 3, also referred to as the executioner caspase, plays a role in inducing cell structural alterations by fragmenting DNA and breaking down proteins in the cytoskeleton [44].

3.6 Investigation of the Expression of Autophagy LC3-II and Bcl-1 Genes

In the study, the number of genes related to autophagy was looked at in MKN-45 cells that were grown on an SFNFs substrate. The cells were divided into two groups: one group was treated with 5-FU, while the other group received no treatment. At 3 and 5 days after treatment, the effect of nanofiber structure on the expression of genes involved in the autophagy pathway was also checked. The results are displayed in Fig. 7. The amounts of LC3-II and Bcl-1 genes were higher in cells treated with 5-FU/ SFNFs carriers after three days than in cells treated with SFNFs alone. This suggests an increase in autophagy (P-value < 0.05). After 5 days, the LC3-II and Bcl-1 genes were more active in cells treated with 5-FU/ SFNFs carriers than in cells treated with only nanofibers (P-value < 0.05).

The results show that SFNFs/5-FU can make MKN-45 cancer cells go through autophagy. The increase in autophagy in MKN-45 cells after exposure to SFNFs containing 5-FU can be attributed to a variety of variables and mechanisms. Autophagy is a cellular mechanism that involves breaking down and reusing damaged or malfunctioning parts of cells. This process can be influenced by a variety of external events, such as drug use [45]. Here are some possible explanations for why these 5-FU/SFNFs might increase autophagy in MKN-45 cells. 5-FU exerts its anticancer effects by interfering with DNA synthesis and

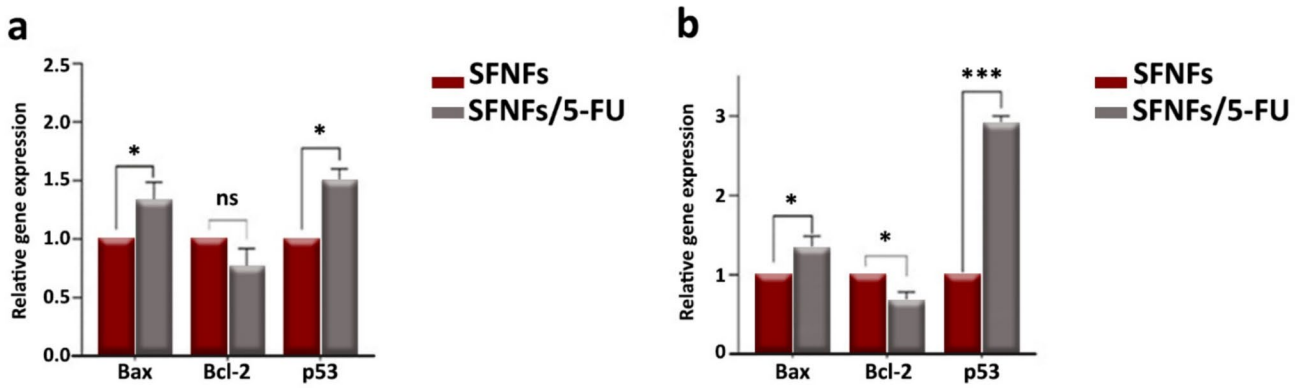

Fig. 6 The results of the expression of apoptosis genes: **a**) Third day, **b**) Fifth day

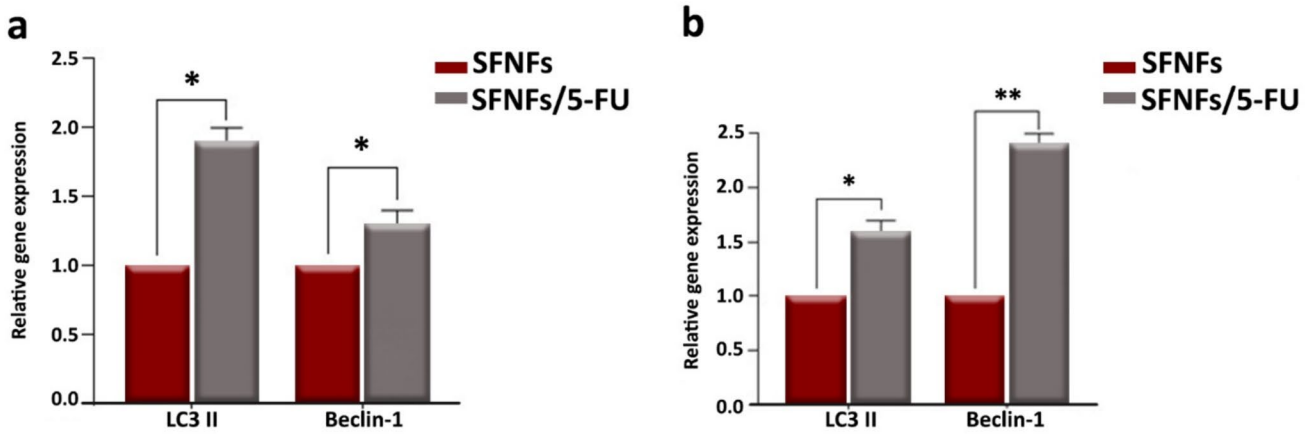

Fig. 7 The results of the expression of autophagy genes: **a**) the third day and **b**) the fifth day

activates RNA transcription, which can lead to the accumulation of damaged DNA and activation of cellular stress responses. This cellular stress can induce autophagy as a defensive process to eliminate impaired components and enhance cell viability [46]. On the other hand, it has been shown that nanofiber structures along with 5-FU administration can increase Bcl-1 and LC3 genes [47]. 5-FU is a chemotherapy drug that interferes with DNA and RNA synthesis in cancer cells, leading to cellular stress. In this regard, Lin et al. have shown that autophagy can be induced by cellular stress to remove damaged cellular components and enhance cell survival. Beclin-1 is a vital protein in the autophagy initiation complex, and its positive regulation is the initial step in the autophagy process, which can ultimately induce autophagy among cancer cells [48]. In summary, it seems that the increase in LC3-II gene expression observed when treating cancer cells with SFNFs/5-FU indicates the activation of autophagy. This response is likely a cellular attempt to cope with the stress caused by 5-FU treatment, remove damaged cellular components, and promote cell survival under adverse conditions.

4 Conclusion

The purpose of this work was to develop a controlled-release drug delivery system for loading 5-FU, a powerful anticancer agent. Using silk fibroin and 5-FU aqueous solution, the nanofibers including the 5-FU drug were successfully prepared in this study. 5-FU can be mostly encapsulated in electrospun materials and showed pH-sensitive release behaviors. SFNFs showed excellent controlled 5-FU delivery at different pHs and the amount of 5-FU release has increased as the pH decreases. This study also found that SFNFs/5-FU can raise the levels of Bax and p53 genes after 3 days, which means that apoptosis has been initiated. Also, after 5 days, it leads to a further increase in Bax and p53 genes, while simultaneously causing a decrease in Bcl-2. On the other hand, it has been shown that SFNFs/ 5-FU administration can increase Bcl-1 and LC3 genes. The increase in this gene expression can indicate the activation of autophagy. This study demonstrates that the combination of SFNFs and 5-FU can effectively treat gastric cancer and stimulate the apoptosis autophagic process. Thus, materials with a nano-fiber structure, especially the SFNFs structure prepared in this study, can release less 5-FU when they meet healthy tissues and more when they meet tumor tissues due to their different pH. These SFNFs have demonstrated their potential as effective delivery structures for cancer treatment because of their high loading capacity and pH-sensitive release profile.

Acknowledgements The authors are grateful from Ardabil University of Medical Sciences.

Authors Contributions MF: Writing—Review & Editing, FR: Methodology, Review & Editing, MJ: Investigation, Methodology, PM: Methodology, Formal analysis, EIJ: Methodology, Validation, HHA: Validation, Investigation, FF: Supervision, Methodology, Validation, Investigation, Resources, Data Curation, Writing—Original Draft, Writing—Review & Editing, Visualization.

Funding The authors are grateful for financial support from Ardabil University of Medical Sciences (grant no: 400000749).

Data Availability No datasets were generated or analysed during the current study.

Declarations

Research Involving Humans and Animals Statement None.

Competing interests The authors declare no competing interests.

Informed Consent Not applicable.

References

1. Jain, S., et al. (2020). pH dependent drug release from drug conjugated PEGylated CdSe/ZnS nanoparticles. *Materials Chemistry and Physics, 240*, 122162.
2. Senapati, S., et al. (2018). Controlled drug delivery vehicles for cancer treatment and their performance. *Signal transduction and targeted therapy, 3*(1), 7.
3. Lai, J., et al. (2024). Alginate-based encapsulation fabrication technique for drug delivery: An updated review of particle type, formulation technique, pharmaceutical ingredient, and targeted delivery system. *Pharmaceutics, 16*(3), 370.
4. Rahmani, H., et al. (2019). Preparation and characterization of silk fibroin nanoparticles as a potential drug delivery system for 5-fluorouracil. *Advanced pharmaceutical bulletin, 9*(4), 601.
5. Shastri, S. S., Varma, P., Kandasubramanian, B. (2024). Enhancing drug delivery with electrospun biopolymer nanofibers. *Biomedical Materials & Devices*, 1–24.
6. Kyser, A. J., et al. (2025). Electrospun nanofibers: Focus on local therapeutic delivery targeting infectious disease. *Journal of Drug Delivery Science and Technology, 104*, 106520.
7. Abdulhussain, R., et al. (2023). Electrospun nanofibers: Exploring process parameters, polymer selection, and recent applications in pharmaceuticals and drug delivery. *Journal of Drug Delivery Science and Technology, 90*, 105156.
8. Gelb, M. B., et al. (2022). Effect of drug incorporation and polymer properties on the characteristics of electrospun nanofibers for drug delivery. *Journal of Drug Delivery Science and Technology, 68*, 103112.
9. Babazadeh-Mamaqani, M., et al. (2024). Photo-responsive electrospun polymer nanofibers: Mechanisms, properties, and applications. *Progress in Materials Science, 146*, 101312.
10. Muratoglu, S., et al. (2024). Electrospun nanofiber drug delivery systems and recent applications: An overview. *Journal of Drug Delivery Science and Technology, 92*, 105342.
11. Nejati-Koshki, K., et al. (2017). Development of Emu oil-loaded PCL/collagen bioactive nanofibers for proliferation and stemness preservation of human adipose-derived stem cells: possible application in regenerative medicine. *Drug Development and Industrial Pharmacy, 43*(12), 1978–1988.
12. Farhaj, S., Conway, B. R., & Ghori, M. U. (2023). Nanofibres in drug delivery applications. *Fibers, 11*(2), 21.
13. Harishchandra Yadav, R., et al. (2024). A review of silk fibroin-based drug delivery systems and their applications. *European Polymer Journal, 216*, 113286.
14. Tran, N. P., Okahisa, Y., & Okubayashi, S. (2025). Chitosan hydrogel containing silk fibroin nanofibrils for controllable properties and its application to drug delivery system. *Next Materials, 6*, 100288.
15. Lu, Q., et al. (2010). Water-insoluble silk films with silk I structure. *Acta biomaterialia, 6*(4), 1380–1387.
16. Jaiswal, C., et al. (2023). Injectable anti-cancer drug loaded silk-based hydrogel for the prevention of cancer recurrence and post-lumpectomy tissue regeneration aiding triple-negative breast cancer therapy. *Biomaterials advances, 145*, 213224.
17. Yu, B., et al. (2023). Research progress of natural silk fibroin and the application for drug delivery in chemotherapies. *Frontiers in Pharmacology, 13*, 1071868.
18. Li, P., et al. (2011). Development of chitosan nanoparticles as drug delivery systems for 5-fluorouracil and leucovorin blends. *Carbohydrate polymers, 85*(3), 698–704.
19. Aydin, R. S. T., & Pulat, M. (2012). 5-Fluorouracil encapsulated chitosan nanoparticles for pH-stimulated drug delivery: Evaluation of controlled release kinetics. *Journal of Nanomaterials, 2012*, 42–42.
20. Liu, J., et al. (2014). pH-sensitive nano-systems for drug delivery in cancer therapy. *Biotechnology advances, 32*(4), 693–710.
21. Li, Z., Huang, J., & Wu, J. (2021). pH-Sensitive nanogels for drug delivery in cancer therapy. *Biomaterials Science, 9*(3), 574–589.
22. Sun, N., et al. (2019). Fabricated porous silk fibroin particles for pH-responsive drug delivery and targeting of tumor cells. *Journal of Materials Science, 54*, 3319–3330.
23. Fathi, M., Akbari, B., & Taheriazam, A. (2019). Antibiotics drug release controlling and osteoblast adhesion from Titania nanotubes arrays using silk fibroin coating. *Materials Science and Engineering: C, 103*, 109743.
24. Fathi, M., et al. (2022). Surface functionalization of Titania Nanotubes arrays and vancomycin controlled release using Silk Fibroin Nanofibers coating. *Journal of Drug Delivery Science and Technology, 71*, 103320.
25. Xi, H., & Zhao, H. (2019). Silk fibroin coaxial bead-on-string fiber materials and their drug release behaviors in different pH. *Journal of Materials Science, 54*, 4246–4258.
26. Zhu, J., et al. (2011). Magnetic polyacrylonitrile-Fe@ FeO nanocomposite fibers-Electrospinning, stabilization and carbonization. *Polymer, 52*(13), 2947–2955.
27. Wang, X. X., et al. (2021). Conductive polymer ultrafine fibers via electrospinning: Preparation, physical properties and applications. *Progress in Materials Science, 115*, 100704.
28. Ji, D., et al. (2024). Electrospinning of nanofibres. *Nature Reviews Methods Primers, 4*(1), 1.
29. Paswan, M., Prajapati, V., & Dholakiya, B. Z. (2022). Optimization of biodegradable cross-linked guar-gum-PLA superabsorbent hydrogel formation employing response surface methodology. *International Journal of Biological Macromolecules, 223*, 652–662.
30. Maitra, J., & Shukla, V. K. (2014). Cross-linking in hydrogels-a review. *Am. J. Polym. Sci, 4*(2), 25–31.
31. Singh, N., et al. (2021). 3-Dimensional cross linked hydrophilic polymeric network "hydrogels": An agriculture boom. *Agricultural Water Management, 253*, 106939.
32. Rizwan, M., et al. (2017). pH sensitive hydrogels in drug delivery: Brief history, properties, swelling, and release mechanism, material selection and applications. *Polymers, 9*(4), 137.
33. Qiu, Y., & Park, K. (2001). Environment-sensitive hydrogels for drug delivery. *Advanced drug delivery reviews, 53*(3), 321–339.
34. Schoeller, J., et al. (2022). pH-responsive electrospun nanofibers and their applications. *Polymer Reviews, 62*(2), 351–399.
35. Foong, C. Y., Wirzal, M. D. H., & Bustam, M. A. (2020). A review on nanofibers membrane with amino-based ionic liquid for heavy metal removal. *Journal of Molecular Liquids, 297*, 111793.
36. Thambi, T., Phan, V. G., & Lee, D. S. (2016). Stimuli-sensitive injectable hydrogels based on polysaccharides and their biomedical applications. *Macromolecular rapid communications, 37*(23), 1881–1896.
37. El-Sawy, N. M., et al. (2020). Radiation development of pH-responsive (xanthan-acrylic acid)/MgO nanocomposite hydrogels for controlled delivery of methotrexate anticancer drug. *International journal of biological macromolecules, 142*, 254–264.
38. Rajabzadeh-Khosroshahi, M., et al. (2022). Chitosan/agarose/graphitic carbon nitride nanocomposite as an efficient pH-sensitive drug delivery system for anticancer curcumin releasing. *Journal of Drug Delivery Science and Technology, 74*, 103443.
39. Guo, Z., et al. (2024). pH-sensitive metal–organic framework carrier decorated with chitosan for controlled drug release. *International Journal of Pharmaceutics, 667*, 124933.
40. Mi, Y., et al. (2024). pH sensitive adriamycin-incorporated nanoparticles self-assembled from amphiphilic chitosan derivatives with enhanced antioxidant and antitumor activities. *Carbohydrate Polymer Technologies and Applications, 7*, 100475.

41. Dhar, D., et al. (2024). Assessment of chitosan-coated zinc cobalt ferrite nanoparticle as a multifunctional theranostic platform facilitating pH-sensitive drug delivery and OCT image contrast enhancement. *International Journal of Pharmaceutics, 654*, 123999.
42. Nita, M. E., et al. (1998). 5-Fluorouracil induces apoptosis in human colon cancer cell lines with modulation of Bcl-2 family proteins. *British journal of cancer, 78*(8), 986–992.
43. Susan, M., et al. (2023). In Vitro Assessment of the Synergistic Effect of Aspirin and 5-Fluorouracil in Colorectal Adenocarcinoma Cells. *Current Oncology, 30*(7), 6197–6219.
44. Brentnall, M., et al. (2013). Caspase-9, caspase-3 and caspase-7 have distinct roles during intrinsic apoptosis. *BMC cell biology, 14*, 1–9.
45. Mizushima, N. (2007). Autophagy: Process and function. *Genes & development, 21*(22), 2861–2873.
46. Blondy, S., et al. (2020). 5-Fluorouracil resistance mechanisms in colorectal cancer: From classical pathways to promising processes. *Cancer science, 111*(9), 3142–3154.
47. Yang, Y., et al. (2024). Application of electrospun drug-loaded nanofibers in cancer therapy. *Polymers, 16*(4), 504.
48 Lin, J., et al. (2015). Hedyotis diffusa Willd. extract suppresses proliferation and induces apoptosis via IL-6-inducible STAT3 pathway inactivation in human colorectal cancer cells. *Oncology Letters, 9*(4), 1962–1970.